INSTITUTE FOR NUCLEAR STUDY
UNIVERSITY OF TOKYO
Tanashi, Tokyo 188
Japan

INS-Rep.-578
March 1986

# Roles of Folding Spin-Orbit Potentials in $^{6,7}\vec{Li}$ Scattering

Y. Sakuragi, M. Kamimura,* M. Yahiro** and M. Tanifuji†

INS-Rep.-578
March 1986

# Roles of Folding Spin-Orbit Potentials in $^{6,7}\vec{Li}$ Scattering

Y. Sakuragi, M. Kamimura,* M. Yahiro** and M. Tanifuji†

Institute for Nuclear Study, University of Tokyo, Tanashi, Tokyo, Japan
*) Department of Physics, Kyushu University, Fukuoka, Japan
**) Shimonoseki University of Fisheries, Shimonoseki, Japan
†) Department of Physics and Research Center of Ion Beam Technology, Hosei University, Tokyo, Japan

Abstract: Spin-dependent interactions responsible for vector analyzing powers in elastic scattering of $^{6,7}\vec{Li}$ are investigated with a special interest in the competition between folding spin-orbit potentials and higher orders of tensor interactions including projectile virtual excitations. For $150 \gtrsim E_{lab} \gtrsim 40$ MeV, they are both important. For $E_{lab} \lesssim 20$ MeV, however, the folding spin-orbit potential cannot be effective because the attenuation due to the projectile excitation and/or the Coulomb barrier prevent the projectile from intruding into the spin-orbit effective area.

Much attention has been paid on the spin-dependent interactions which generate vector and tensor analyzing powers in scattering of polarized $^{6,7}$Li ions. For the $^{7}\vec{\text{Li}}$ scattering from $^{58}$Ni at 14.2 and 20.3 MeV, the following features (i)~(iii) of the interactions has become well-known [1,2,3], especially through the coupled-channel (CC) calculations [2,3] with cluster-folding tensor interactions which cause the projectile excitation to the $1/2^-$ bound state ($\ell$=1) at $E_x$=0.478 MeV and the $7/2^-$ and $5/2^-$ resonance states ($\ell$=3) at $E_x$=4.63 and 6.68 MeV as well as the reorientation of the $3/2^-$ ground state ($\ell$=1): (i) The large tensor analyzing powers are given chiefly by the folding tensor potential of the ground state which has a large quadrupole moment, whereas the contribution of the projectile virtual excitation is small. (ii) The vector analyzing power, which is rather small, i.e. $|iT_{11}(\theta)| \lesssim 0.05$, is attributed to the second- and higher-order effects of the folding tensor potential and those of the tensor coupling to the excited states. (iii) The contribution of the folding spin-orbit potential to the vector analyzing power is negligibly small and even has the opposite sign to the observed. Similarly, as for $^{6}\vec{\text{Li}}$+$^{58}$Ni at 20.0 MeV, it was found [2,3] that the contribution of the folding spin-orbit potential to the vector analyzing power is negligible, and the vector analyzing power is explained by the second- and higher-order effect of the tensor interactions which excite the projectile to the $3^+$, $2^+$ and $1^+$ resonance states ($\ell$=2) at $E_x$=2.19, 4.31 and 5.65 MeV, respectively.

For $^{6,7}\vec{\text{Li}}$ scattering from <u>light targets</u> at ~20 MeV, however, there remains somewhat puzzling problem about the spin-dependent interactions which are responsible for explaining the observed vector analyzing power. Namely, the gross feature of the rather large, observed vector analyzing power, $|iT_{11}(\theta)| \lesssim 0.4$, for the $^{7}\vec{\text{Li}}$+$^{12}$C scattering at 21.1 MeV [4] is fairly well reproduced by the single-channel ($3/2^-$) calculation in which the central potential is searched within the Woods-Saxon geometry but the spin-orbit potential is fixed to the cluster-folding one (no tensor potential is included). A similar single-channel calculation appeared in ref.[4] fits to the analyzing-power data, where all parameters are fully varied. Such considerable successes are in a striking contrast to the case of $^{7}\vec{Li}+^{58}Ni$ scattering at the similar energy. On the other hand, however, in our previous work [5] the same data were also reproduced with the CC calculation mentioned above; the vector analyzing power was attributed to the same type of tensor interactions as in $^{7}\vec{Li}+^{58}Ni$, and the calculated vector analyzing power was affected little by the inclusion (or neglect) of the folding spin-orbit potential. How can the puzzle of these contradicting conclusions be solved? A similar problem will happen in $^{6}\vec{Li}+^{16}O$ at 22.8 MeV when a single-channel calculation with the folding spin-orbit potential [6] is compared with our previous CC calculation including the $3^{+}$, $2^{+}$ and $1^{+}$ excited states of $^{6}Li$ [5].

In this letter, we shall solve this puzzling problem on the vector analyzing power in the $^{6,7}\vec{Li}$ scattering at $E_{lab}\simeq 20$ MeV and discuss, in a wide range of targets and energies, the role of the folding spin-orbit potential in the presence of the tensor interactions, a part of which induces the virtual excitation of the projectile. Coupling with excited states of the projectile is treated in the CC framework [2] as mentioned above. Internal states of the $^{7}Li$($^{6}Li$) nucleus are described by an $\alpha$-t($\alpha$-d) cluster model. The method of calculating the interactions between the projectile and the target has been described in detail in ref.[2], which is followed by the present calculation. For the $^{7}Li$ case, for example, the cluster folding interaction for the transition of the projectile between i-th state and j-th state is given by folding the $\alpha$-target and t-target optical potentials into the two states. The $^{7}Li$-target spin-orbit potential is generated by folding the spin-orbit part of the t-target potential into the ground state of $^{7}Li$. Both the third-rank tensor interaction and the spin-orbit coupling to the excited states are ignored to simplify the conclusion. Actually, they are not important at all for the cases studied in the present note. It is to be noted that there is no adjustable parameter left in the cluster-folding interactions once the optical potentials are chosen from literature. For simplicity in the discussions below, we shortly refer to the folding central and spin-orbit potentials as "C" and "LS", respectively, and the tensor interactions as "T". Here, T indicates both the folding tensor potential and the tensor coupling interactions.

Figure 1 shows the observed and calculated vector analyzing powers, $iT_{11}$, for $^{7}\vec{Li}+^{12}C$ at 21.1 MeV. The $\alpha-^{12}C$ and $t-^{12}C$ optical potentials are taken from refs. [7] and [8], which reproduce the observed data for tensor analyzing powers very well [5] by the CC method of this note. The single-channel calculation with C+LS is given by the upper-most dotted curve which may be considered to represent the pure contribution of the folding spin-orbit potential to $iT_{11}$ and fits fairly well the gross behaviour of the observed $iT_{11}$. The other three parts of Fig.1 show the results of the CC calculations with C+T+LS by the solid curves and those with C+T by the dashed ones; the projectile states included in the three calculations are the $3/2^{-}$ (ground) state only, the $3/2^{-}$ and $1/2^{-}$ states and the $3/2^{-}$, $1/2^{-}$, $7/2^{-}$ and $5/2^{-}$ states, respectively, from top to bottom. The difference between the solid and dashed curves in the individual part of Fig.1 is identified as the contribution of the folding spin-orbit potential in the presence of the tensor interactions. It is clearly seen that the contribution decreases quickly with the increase of the projectile excited channels coupled. In spite of the fit to the rather large $iT_{11}$ by the single-channel calculation with C+LS only, the effect of LS is almost completely attenuated by the virtual excitations of the $^{7}Li$ projectile to the $1/2^{-}$, $7/2^{-}$ and $5/2^{-}$ states. It will be worth while noting that a similar attenuation of the effect of LS is also seen in third-rank tensor analyzing powers.

The mechanism of this attenuation may be understood as follows: As is seen in Fig.2 LS is of a volume type and the range is much shorter than that of T which causes the excitation of the projectile in the surface. Therefore, the incident wave will hardly touch the nuclear interior where LS is effective. In fact, it is found that when the coupling to the excited states is switched on, an additional absorption is particularly induced on the elastic-scattering partial waves with small angular momenta which correspond to the range of LS. For the case of heavier targets such as $^{58}$Ni, the short-ranged LS is already screened by the high Coulomb barrier even in the single channel calculation with C+LS. On the other hand, for the case of light targets, the barrier is low enough for the incident wave to reach LS as long as T is neglected; it may then be said that, on account of neglecting T, the single-channel model with LS plus a phenomenological central potential could luckily account for the magnitude of the observed $iT_{11}$. Due to lack of T, however, this model cannot explain at all the large tensor analyzing powers observed; the second-order contribution of LS to the tensor analyzing powers is negligibly small. Therefore, this model is not suitable for a consistent understanding of the whole observables in the $^{7}\vec{\text{Li}}$ scattering. On the other hand, the present CC model can account for the tensor analyzing powers by T and simultaneously vector analyzing power by the second- and higher-order effect*) of T. As long as T is ignored, the role of LS looks

---

*) If one tries to simulate this effect of T on $iT_{11}$ with the use of an effective spin-orbit (SO) potential in a single-channel framework, he will obtain a potential which is located in the surface region where T is active. But, a further introduction of some tensor potential is necessary to explain the tensor analyzing powers, and this potential will also contribute substantially to $iT_{11}$. Hence, the SO potential which explains $iT_{11}$ in the presence of the tensor potential will much differ from the effective SO potential mentioned above. One should be careful of this point when he intends to discuss about effective SO potentials.

significant for light targets, but it is fatally attenuated by the presence of T in actual case. This warns us that it is not always adequate to consider vector analyzing power to reflect principally the strength of a spin-orbit potential in scattering of polarized ions.

For the scattering of $^{6}\vec{Li}$ from $^{16}O$ at 22.8 MeV, the analysi. same as the above is made and a similar conclusion is obtained for the roles of LS and T in the explanation of the vector analyzing power.

Since the strength of the spin-orbit potential is propotional to the angular momentum, it is expected that the role of LS in vector analyzing power becomes important when the incident energy is increased. In fact, a substantial effect of LS is seen in $^{7}\vec{Li}+^{120}Sn$ at 44 MeV. Figure 3 shows the cross section and the vector analyzing power of the scattering given by the recent experiment at Heidelberg [9] and by the present CC calculation where the $3/2^-$, $1/2^-$, $7/2^-$ and $5/2^-$ states of the $^{7}Li$ projectile are taken into account. The α-target and t-target optical potentials are taken from refs. [10] and [11], respectively. (This type of CC calculation [12] was found to reproduce well the second- and third-rank tensor analyzing powers observed [9] as well as the vector one.) The pure contribution of LS to $iT_{11}$ is represented with the dotted curve given by the single-channel ($3/2^-$) calculation, and it is rather large in contrast with the negligible role of LS in $^{7}\vec{Li}+^{58}Ni$ at 20.3 MeV. The contribution of T to $iT_{11}$ in the four-channel calculation without LS is shown by the dashed curve, which is about 1.5 times as large as the pure contribution of LS in magnitude with the opposite sign. The solid curve in Fig.3 shows the coherent contribution of T and LS in the four-channel calculation and $iT_{11}$ is nearly the simple sum of the dotted and dashed curves. We thus note that in $^{7}\vec{Li}+^{120}Sn$ scattering at 44 MeV the role of LS is evident (amounting to about 2/3 of that of T) and is still significant even in the presence of T.

For $^{7}Li+^{12}C$ scattering at 48 MeV where no measurement of the polarization quantities has been made so far, a present type of CC calculation [12] reproduces well the observed cross sections [13] of the elastic scattering and inelastic one to the projectile and target excited states. The calculation predicts that the contribution of LS to the vector analyzing power is dominant for $\theta_{cm} \lesssim 40°$ though it is still smaller than the contribution of T for $\theta_{cm} \gtrsim 50°$. For $^6Li+^{12}C$ scattering at 150 MeV, a present type of CC calculation [14] reproduces the observed elastic cross section and shows that the individual contributions of LS and T to $iT_{11}$ are very similar to each other with the same positive sign and a weak angular dependence (a half of the contribution of T comes from the virtual projectile breakup into the non-resonant continuum states); the coherent contribution of LS and T is predicted to be typically $iT_{11}=0.12$ and 0.20 at two peaks of the differential cross section ($\theta_{cm}=12°$ and 20°, respectively). This estimation is consistent with the double-scattering experiment of $^6Li$ by $^{12}C$ at 150 MeV [14]; the observed value is $|iT_{11}| = 0.02 \left\{ \begin{matrix} +\ 0.11 \\ -\ 0.02 \end{matrix} \right\}$ at $\theta_{cm}= (12 \pm 1.5)°$.

We have studied the spin-dependent interactions which are responsible for the vector analyzing power of the $^{6,7}\vec{Li}$ scattering. Special attention has been paid on the competition between the folding spin-orbit potential and the higher-order effect of the tensor interactions including the projectile excitations. For $E_{lab} \gtrsim 40$ MeV, both are comparably important for the vector analyzing powers. For $E_{lab} \lesssim 20$ MeV, however, the folding spin-orbit potential can be neglected; it is interesting that for light targets the pure contribution of the folding spin-orbit potential looks rather large if the tensor interactions are neglected, but the contribution is fatally attenuated by the presence of the strong tensor coupling to the projectile excited channels.

## References


1) E. Steffence, Proc. Fifth Int. Symp. Polar. Phenom. Nucl. Phys., Santa Fe, 1980, p.1001,
Z. Moroz et al., Nucl. Phys. A381 (1982) 294.

2) H. Ohnishi, M. Tanifuji and H. Noya, Phys. Lett. 108B (1981) 83,
H. Ohnishi, M. Tanifuji, M. Kamimura and M. Yahiro, Phys. Lett. 118B (1982) 16,
H. Ohnishi, M. Tanifuji, M. Kamimura, Y. Sakuragi and M. Yahiro, Nucl. Phys. A415 (1984) 271

3) H. Nishioka, R.C. Johnson, J.A. Tostevin and K.-I. Kubo, Phys. Rev. Lett. 48 (1982) 1795,
H. Nishioka, J.A. Tostevin, R.C. Johnson and K.-I. Kubo, Nucl. Phys. A415 (1984) 230.

4) Z. Moroz et al., Nucl. Phys. A417 (1984) 498.

5) Y. Sakuragi, M. Kamimura, M. Yahiro and M. Tanifuji, Phys. Lett. 153B (1985) 372.

6) W. Weiss et al., Phys. Lett. 61B (1976) 237.

7) T. Terasawa, M. Tanifuji and O. Mikoshiba, Nucl. Phys. A203 (1973) 225.

8) D. Fick et al., Phys. Rev. C29 (1984) 324.

9) G. Tungate et al., Jahrensbericht 1984 Max-Planck-Institut für Kernphysik Heidelberg, p.106,
Z. Moroz, Proc. Sixth Int. Symp. Polar. Phenom. Nucl. Phys., Osaka, 1985, J. Phys. Soc. Jpn. 55 (1986) Suppl. p.221.

10) C.M. Perey and F.G. Perey, Atom. Data and Nucl. Data Tables 13 (1974) 293.

11) R.A. Hardekopf et al., Phys. Rev. C21 (1980) 906.

12) M. Kamimura, Y. Sakuragi, M. Yahiro and M. Tanifuji, Proc. Sixth Int. Symp. Polar. Phenom. Nucl. Phys., Osaka, 1985, J. Phys. Soc. Jpn. 55 (1986) Suppl. p.205.

13) A.F. Zeller et al., Nucl. Phys. A323 (1979) 477.

14) M. Tanaka, T. Yamagata, K. Yuasa, S. Nakayama, M. Inoue, Y. Sakuragi, M. Kamimura, H. Goto, K. Katori, M. Yanagi and H. Ogata, Proc. Sixth Int. Symp. Polar. Phenom. Nucl. Phys., Osaka, 1985, J. Phys. Soc. Jpn. 55 (1986) Suppl. p.764,
M. Tanaka et al., private communication.

Figure captions

Fig.1. Coupled-channel calculation of the vector analyzing power for $^{7}\vec{Li}+^{12}C$ at 21.1 MeV. The upper-most curve shows the pure contribution of the folding spin-orbit potential (LS). The curves below show results of the CC calculations with LS (solid curves) and without LS (dashed curves). The data are taken from ref.[4].

Fig.2. Geometry of the folding spin-orbit potential (LS), real part of the folding central potential (C) and real part of the tensor coupling potential (T) between the $3/2^-$ and $1/2^-$ states for $^{7}Li+^{12}C$ at 21.1 MeV.

Fig.3. Cross section and vector analyzing power for $^{7}\vec{Li}+^{120}Sn$ at 44 MeV. The solid and dashed curves are given by the four-channel CC calculations with and without the folding spin-orbit potential (LS), respectively. The dotted curve shows the result of the single-channel calculation with LS but without the folding tensor potential. The data are taken from ref.[9].

Fig. 1

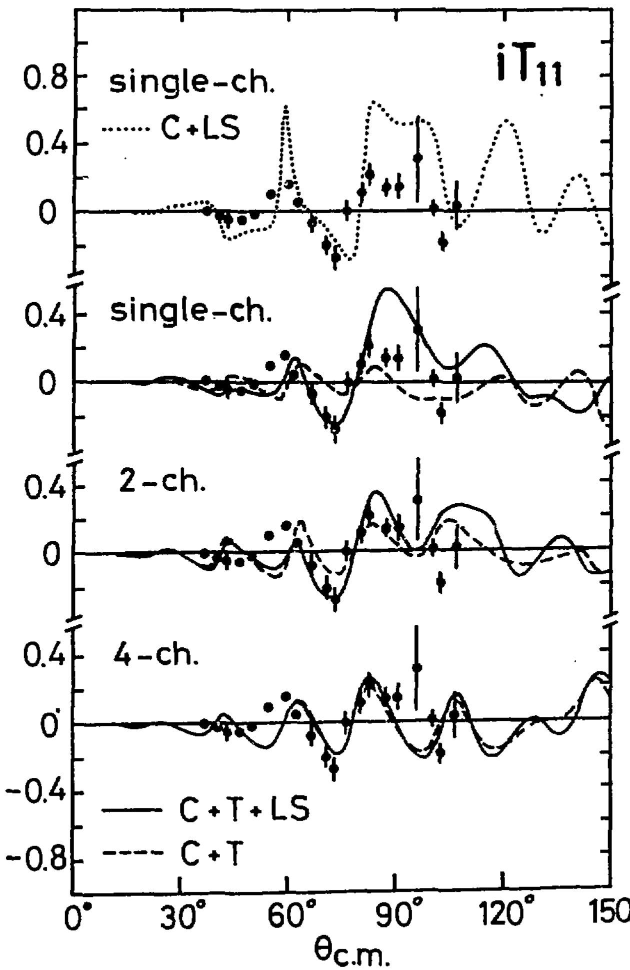

iT11
single-ch.
······ C+LS
single-ch.
2-ch.
4-ch.
— C+T+LS
---- C+T
0.8
0.4
0
-0.4
-0.8
0°
30°
60°
90°
120°
150°
θc.m.

Fig. 2

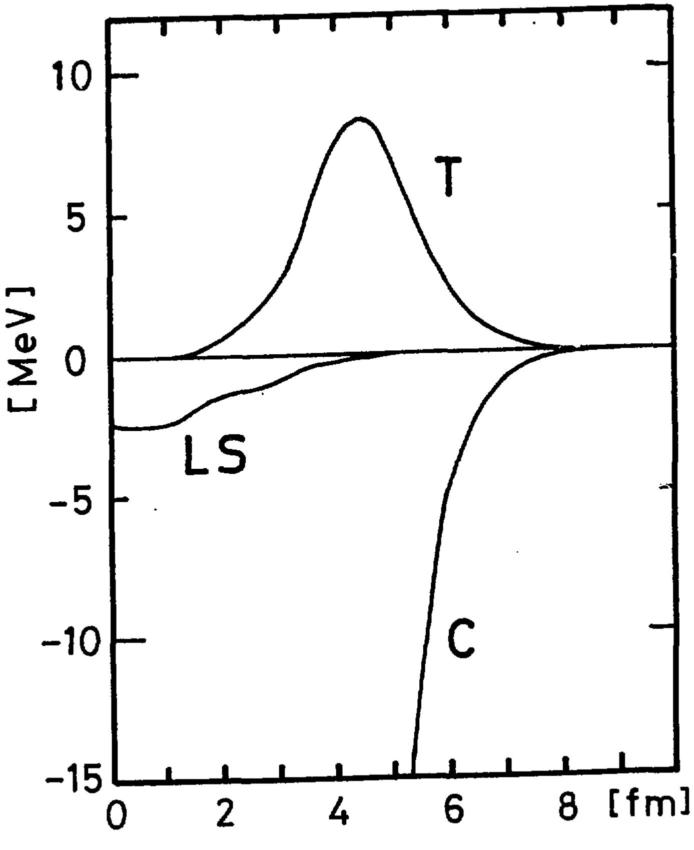

Fig. 3

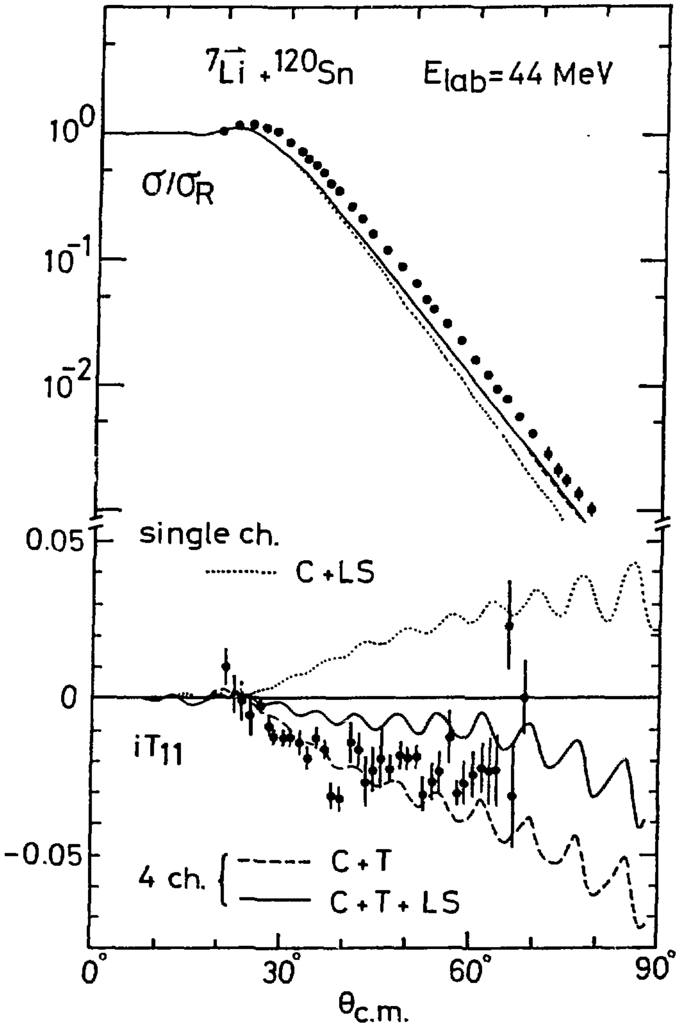

$^7\vec{Li} + ^{120}Sn$
$E_{lab}$=44 MeV
$10^0$
$\sigma/\sigma_R$
$10^{-1}$
$10^{-2}$
0.05
single ch.
C + LS
0
$iT_{11}$
-0.05
4 ch.
C + T
C + T + LS
0°
30°
60°
90°
$\theta_{c.m.}$